A Perfectly Matched Layer Approach to the Linearized Shallow Water Equations Models

I. M. NAVON

Department of Mathematics, and School of Computational Science and Information Technology, The Florida State University, Tallahassee, Florida

B. NETA

Department of Mathematics, Naval Postgraduate School, Monterey, California

M. Y. HUSSAINI

School of Computational Science and Information Technology, The Florida State University, Tallahassee, Florida

ABSTRACT

A limited-area model of linearized shallow water equations (SWE) on an f plane for a rectangular domain is considered. The rectangular domain is extended to include the so-called perfectly matched layer (PML) as an absorbing boundary condition. Following the proponent of the original method, the equations are obtained in this layer by splitting the shallow water equations in the coordinate directions and introducing the absorption coefficients. The performance of the PML as an absorbing boundary treatment is demonstrated using a commonly employed bell-shaped Gaussian initially introduced at the center of the rectangular physical domain.

Three typical cases are studied:

- A stationary Gaussian where adjustment waves radiate out of the area.
- A geostrophically balanced disturbance being advected through the boundary parallel to the PML. This advective case has an analytical solution allowing one to compare forecasts.
- The same bell being advected at an angle of 45° so that it leaves the domain through a corner.

For the purpose of comparison, a reference solution is obtained on a fine grid on the extended domain with the characteristic boundary conditions. Also computed are the rms difference between the 48-h forecast and the analytical solution as well as the 48-h evolution of the mean absolute divergence, which is related to geostrophic balance. The authors found that the PML equations for the linearized shallow water equations on an f plane support unstable solutions when the mean flow is not unidirectional. Use of a damping term consisting of a 9-point smoother added to the discretized PML equations stabilizes the PML equations. The reflection/transmission is analyzed along with the case of instability for glancing propagation of the bell disturbance. A numerical illustration is provided showing that the stabilized PML for glancing bell propagation performs well with the addition of the damping term.

1. Introduction

In a limited-area numerical weather prediction model, the lateral boundaries are not physical boundaries, and they require artificial boundary conditions so that the problem is well posed and the solution in the limited area remains uncontaminated and consistent with the global solution. As such, the treatment of lateral boundaries with the nonreflecting or absorbing boundary conditions has been the subject of continuing interest since the early days of numerical weather prediction.

Several good reviews are available on the topic of both physical and artificial boundary conditions (Turkel 1983; Givoli 1991; McDonald 1997; Tsynkov 1998). D. Givoli and I. Harari edited a special issue of *Computer Methods in Applied Mechanics and Engineering* (1998, vol. 164, nos. 1–2) on the subject of boundary conditions for exterior wave propagation problems. Turkel (1983) provided an early review on the outflow boundary conditions in the context of computational aerodynamics. Givoli (1991) reviews nonreflecting boundary conditions for the wave problems and discusses local and nonlocal boundary conditions for physical and ar-

Corresponding author address: Dr. I. M. Navon, Dept. of Mathematics and School of Computational Science and IT, The Florida State University, Tallahassee, FL 32306-4120.
E-mail: navon@csit.fsu.edu

tificial boundaries in the context of problems from different disciplines. McDonald's (1997) review is confined to lateral boundary conditions for operational regional forecast models. Kalnay (2001) presents the state of art of limited-area boundary conditions as used in meteorology. The most comprehensive survey to date of artificial boundary conditions is given by Tsynkov (1998). He provides a comparative assessment of the current methods for constructing the artificial boundary conditions and divides them into two categories—local and global artificial boundary conditions. Global artificial boundary conditions are so called because they involve integral transforms along the artificial boundary. For example, the approaches of Givoli and Keller (1989) typify the global artificial boundary conditions. Such boundary conditions seem to work only in specific geometries. In addition, discretization by a finite-element method results in the filling of dense blocks in an otherwise sparse system. On the other hand, local artificial boundary conditions preserve the sparsity of the problem, for example, Sommerfeld radiation condition and the traditional characteristic boundary conditions. Typical examples of local approaches to artificial boundary conditions are those of Gustafsson and Sundström (1978) and Engquist and Majda (1977, 1979). The so-called transparent boundary conditions of McDonald (2001a,b; 2002) and of Holstad and Lie (2001) and Lie (2001) applied to the shallow water equations also belong to this category.

The buffer/sponge layer consists in surrounding the truncated physical domain with a zone in which nonphysical equations are employed to filter or damp incident waves so that there is minimal reflection into the physical domain of interest (see Kar and Turco 1995). The boundary relaxation scheme of Davies (1976, 1983) is such an approach, and it is most frequently used for limited-area forecasting using mesoscale models.

The perfectly matched layer (PML) method recently introduced by Berenger (1994) as an absorbing boundary condition in the context of electromagnetic wave propagation has the property of absorbing incident waves irrespective of their frequency and orientation. The parameters of the PML are chosen such that the wave either never reaches the external boundary, or, even if it reaches the boundary and reflects back, its amplitude is negligibly small by the time it reaches the interface between the absorbing layer and interior domain. Hu (1996a) was the first to apply the PML approach to aeroacoustic problems using the linearized Euler equations, then extending his work to nonuniform mean flow for the nonlinear Euler equations (Hu 1996b; Clement 1996; Karni 1996; Kosloff and Kosloff 1986; Collino 1997; Hayder et al. 1999; Hayder and Atkins 1998). The work of Hayder et al. (1999) is the first to demonstrate the viability of the PML method in the application to nonlinear Euler equations. A preliminary work of Darblade et al. (1997) implements the PML method to the linearized shallow water equations model in oceanography.

Hu (2001) presents a new stable PML formulation for the linearized Euler equations in unsplit physical variables and provides a modification to render the proposed scheme strongly well posed by the addition of arbitrarily small terms. Abarbanel and Gottlieb (1997) provide the general mathematical analysis of the PML method while Abarbanel et al. (1999) provide a well-posed version of PML for advective acoustics. Abarbanel and Gottlieb (1998) provide the mathematical framework for use of PML in computational acoustics. The well-posedness of PML for linearized Euler equation and for the Cauchy problem is discussed in Rahmouni (2000) and Metral and Vacus (1999), respectively. The PML approach has been shown to provide significantly better accuracy than most other artificial boundary conditions in many applications.

This paper is organized as follows. In section 2, we introduce the PML approach to the linearized two-dimensional shallow water equations on an f plane for the purpose of analysis. Using a MAPLE symbolic manipulator we obtain a dispersion relation for the linearized PML split shallow water equations system. In section 3 we provide a description of the numerical testing using a widely employed bell-shaped Gaussian (McDonald 2000) at the center of the domain. The first test consists of an adjustment case that is not in geostrophic balance, and we compare the PML results with its known asymptotic solution. We then proceed to test an advective case of the bell-shaped Gaussian propagating in parallel to the PML. This case has an analytical solution with which we can compare our forecasts in terms of rms error as well as the vanishing of the mean absolute divergence. Note that since the system is in geostrophic balance, the analytical divergence on a constant f plane is always zero. This is followed by a test of propagation of the bell-shaped Gaussian at an angle with the PML yielding unstable solutions of the PML equations (see also Hu 1996a; Tam et al. 1998). An analysis is carried out to understand and explain the underlying reasons for the instability. Application of a 9-point Laplacian filter stabilizes the PML.

2. The perfectly matched layer methodology

In this section we will briefly present the framework of the PML method for the linearized shallow water (SW) equations on an f plane.

a. Linearized SW equations on an f plane

The 2D linearized shallow water model on an f plane is of the form

$$\frac{\partial}{\partial t}u + U\frac{\partial}{\partial x}u + V\frac{\partial}{\partial y}u + \frac{\partial}{\partial x}\phi - fv = 0, \quad (1)$$

$$\frac{\partial}{\partial t}v + U\frac{\partial}{\partial x}v + V\frac{\partial}{\partial y}v + \frac{\partial}{\partial y}\phi + fu = 0, \quad (2)$$

$$\frac{\partial}{\partial t}\phi + U\frac{\partial}{\partial x}\phi + V\frac{\partial}{\partial y}\phi + \Phi\left(\frac{\partial u}{\partial x} + \frac{\partial v}{\partial y}\right) = 0, \quad (3)$$

where $U = U_{\text{mean}}$ and $V = V_{\text{mean}}$ are constants, and Φ is the mean geopotential height. If we put $V = 0$, $f = 0$, and scale the geopotential, we get the linearized Euler equations used by Hu (1996b). Thus the results of Hu (1996b) are applicable to this form of the linearized SW equations (not including Coriolis).

b. The split-PML linearized shallow water equations on the f plane

The inclusion of the Coriolis factor in the linearized shallow water equations about (U, V) requires the following modification of the PML split form given by Hu (1996b):

$$\frac{\partial u_1}{\partial t} + U\frac{\partial u}{\partial x} + \frac{\partial \phi}{\partial x} = -\sigma_x u_1,$$

$$\frac{\partial u_2}{\partial t} + V\frac{\partial u}{\partial y} = -\sigma_y u_2, \qquad \frac{\partial u_3}{\partial t} - fv = 0,$$

$$\frac{\partial v_1}{\partial t} + U\frac{\partial v}{\partial x} = -\sigma_x v_1,$$

$$\frac{\partial v_2}{\partial t} + V\frac{\partial v}{\partial y} + \frac{\partial \phi}{\partial y} = -\sigma_y v_2, \qquad \frac{\partial v_3}{\partial t} + fu = 0,$$

$$\frac{\partial \phi_1}{\partial t} + \Phi\frac{\partial u}{\partial x} + U\frac{\partial \phi}{\partial x} = -\sigma_x \phi_1,$$

$$\frac{\partial \phi_2}{\partial t} + \Phi\frac{\partial v}{\partial y} + V\frac{\partial \phi}{\partial y} = -\sigma_y \phi_2. \qquad (4)$$

In the above, the coefficients σ_x and σ_y have been introduced for the absorption of waves in the PML. We will refer to them as absorption coefficients in this work, and they will be assumed to be nonnegative. In general, these coefficients are not constant (see later) but in the analysis in this section will assume constant absorption coefficients. We notice that when

$$\sigma_x = \sigma_y = 0 \qquad (5)$$

we are reduced to the original linearized 2D shallow water equations with

$$u = u_1 + u_2 + u_3, \qquad (6)$$

$$v = v_1 + v_2 + v_3, \qquad (7)$$

$$\phi = \phi_1 + \phi_2. \qquad (8)$$

The spatial derivatives involve only the total fields of u, v, and ϕ, which are assumed to be continuous at the

TABLE 1. Interface types involving the PML and interior domains.

PML	$(0, \sigma_y)$	(σ_x, σ_y)
	$(0, 0)$	$(\sigma_x, 0)$
	Interior	PML

interface between the interior domain and the PML. Two types of interfaces are being created, namely, the interfaces between the interior domain and the PML domain and those between two adjacent PML domains (see Table 1).

A similar approach was used for the linearized shallow water equations in oceanography by Darblade et al. (1997). If we use the split suggested by Hu (1996a), the linearized system will have a solution $u_2 = 0$, and be as if we did not split the u variable in the PML.

The dispersion relation (see Darblade 1997) between possibly complex wave vector (k_x, k_y) and possibly complex frequency ω can be obtained (using the MAPLE symbolic manipulator):

$$-\omega^2 W_x^3 W_y^3 Z[\Phi(X^2 + Y^2) - F^2 + Z^2] = 0, \quad (9)$$

where

$$Z = 1 + iUX, \qquad (10)$$

$$W_x = \sigma_x - i\omega, \qquad W_y = \sigma_y - i\omega, \qquad (11)$$

$$X = \frac{k_x}{W_x}, \qquad Y = \frac{k_y}{W_y}, \qquad F = \frac{f}{\omega}. \quad (12)$$

These equations imply that W_x and W_y are not zero, but the vanishing of these variables is included in (9). In the case in which we include the terms with V, the dispersion relation will be the same except for Z, which will depend on V as follows:

$$Z = 1 + iUX + iVY. \qquad (13)$$

The solution of the dispersion equation (9) can have stable and unstable solutions.

c. Reflection and transmission at an interface between two domains

We quote here the necessary conditions for perfect transmission of plane waves at the interface between two distinct domains, D_1 and D_2. This includes the interface between the interior limited-area domain and the PML domain (see Darblade 1997).

The linearized SW equations can be viewed as the split-field PML linearized SW equations, with both absorption coefficients being zero across an interface normal to x and y between an interior domain and a PML domain.

Following Darblade (1997), we let the interface Γ between the two domains D_1 and D_2 be a line $x = x_0$. Let σ_{x_i}, σ_{y_i}, $i = 1, 2$ be the absorption coefficients in the x, y directions in D_i. The variables u, v, ϕ are continuous across the interface Γ. The necessary conditions

for the perfect transmission at the interface of a plane wave is of the form

$$\psi = \Psi_0 e^{i(k_x x + k_y y - \omega t)},$$

where $\psi = (u_1, u_2, u_3, v_1, v_2, v_3, \phi_1, \phi_2)$ is the solution of (4) if

1) the triplet (ω, k_x, k_y) satisfies the dispersion equation (9)
2) the amplitudes Ψ_0 are the solution of the linear homogeneous system for which the determinant is the dispersion equation (9).

The sufficient condition for perfect transmission is $\sigma_{y_1} = \sigma_{y_2}$. Note that if the interface is parallel to the y axis, the condition becomes $\sigma_{x_1} = \sigma_{x_2}$.

3. Numerical testing

A 2D linearized shallow water equations solver based on the explicit time-differencing scheme of Miller–Pearce is used (see appendix of Miller and Pearce 1974). This scheme is implemented on a nonstaggered grid but provides a fair comparison since all methods are tested using the same discretization. The scheme has a Courant–Friedrichs–Lewy (CFL) stability condition

$$\Delta t \leq \frac{\sqrt{(\Delta x)^2 + (\Delta y)^2}}{\sqrt{\Phi}\sqrt{2}}.$$

Spatial differencing of the linearized shallow water equations was carried out on a rectangular domain of 141×141 grid points, with a uniform spatial horizontal grid length of $\Delta x = \Delta y = 100$ km. We used values of $H = h_{av} = 5000$ m and a time step of $\Delta t = 120$s. At the outer boundary of the PML domain we apply characteristic boundary conditions. On the boundary line we imposed $\phi - \sqrt{\Phi}v_N$ at all points and v_T at the inflow points, where v_N and v_T are the outward normal and tangential components of velocity, respectively.

We compared the results with a control simulation computed on a much larger domain of 400 by 400 grid points, which is not affected by the boundary conditions for the integration time span. The PML domain contains points (x, y) such that $50 < |x|/\Delta x < 70$ and $50 < |y|/\Delta y < 70$.

a. Testing adjustment case

We investigated the permeability of the boundaries for the PML case for the linearized shallow water equations. The initial state considered is with $\nabla\phi(x, y, 0) \neq 0$ and $u(x, y, 0) = v(x, y, 0) = 0$. Since the system is not in geostrophic balance, the system radiates adjustment gravity waves and it will adjust to a balanced state given by the streamfunction $\psi(x, y)$, which satisfies the equation

$$\left(\frac{\partial^2}{\partial x^2} + \frac{\partial^2}{\partial y^2} - \frac{f^2}{\Phi}\right)\psi(x, y) = -\frac{f^2}{\Phi}\phi(x, y, 0). \quad (14)$$

See Gill (1982, section 7.2.2) for details as well as McDonald (2002). For all our numerical tests we used $\Delta x = \Delta y = 100$ km and $L_x = L_y = 10\,000$ km. In all the tests conducted, we used $\Phi = (5000$ m) g, and $\hat{\phi} = (500$ m) g. The experiment starts with a bell-shaped Gaussian at the center of the domain

$$\phi(x, y, 0) = \Phi + \hat{\phi}\exp\left[-\left(\frac{x - L_x/2}{L_x/10}\right)^2\right]$$

$$\times \exp\left[-\left(\frac{y - L_y/2}{L_y/10}\right)^2\right], \quad (15)$$

with $u(x, y, 0) = v(x, y, 0) = 0$, and the advecting velocities U, V are also set to zero. The adjustment process radiates away gravity waves from the center of the domain.

The absorption coefficients are varied gradually inside the PML. Typically, one uses

$$\sigma_x = \sigma_m\left|\frac{x - x_l}{D}\right|^\gamma, \qquad \sigma_y = \sigma_m\left|\frac{y - y_l}{D}\right|^\gamma, \quad (16)$$

where x_l, y_l denote the location where the PML starts, D is the depth of the layer, and γ is a constant (see Hu 1996b). A PML of only $20\Delta x$ depth, was used where the parameters governing the spatial variation of σ_x, σ_y for the absorbing layer were $\gamma = 3$ and $\sigma_m = 0.0018$. The asymptotic state arrived at by solving the balance equation (14) is compared as in McDonald (2002) with the 48-h forecasts to assess the transparency of the boundaries.

We display in Fig. 1 various stages of the adjustment process showing that $h(x, y, t)$ is always circularly symmetric. In Fig. 1a we show the initial condition, a Gaussian bell at the center of the domain. In Fig. 1b one can see the solution after 6 h. Figure 1c gives the solution after 42 h. The rms differences between a 48-h forecast and the asymptotic solution given by the balanced state are provided in Table 2. This balanced state is arrived at by solving (14) with $\phi(x, y, 0)$ given by (15) and $\psi = (5000$ m)g on the boundary is not displayed, but is visually identical to the 48-h forecast shown in Fig. 1c.

These results show that the boundaries are almost transparent to the adjustment waves; that is, the waves exit without reflection. The forecast is almost identical to the asymptotic balanced state described in McDonald (2002).

A graph of the mean absolute divergence (in s^{-1}) multiplied by 10^8 is displayed in Fig. 2 for the propagation of the bell-shaped Gaussian for the case of adjustment. The absolute value of divergence is displayed for three cases: the small domain with PML case, small domain without PML, and large domain. The results of the PML case and the large domain are practically indistinguishable for up to $t = 48$ h. The case of no PML shows large deviations starting at $t = 14$ h but later settles to the common value at about $t = 42$ h.
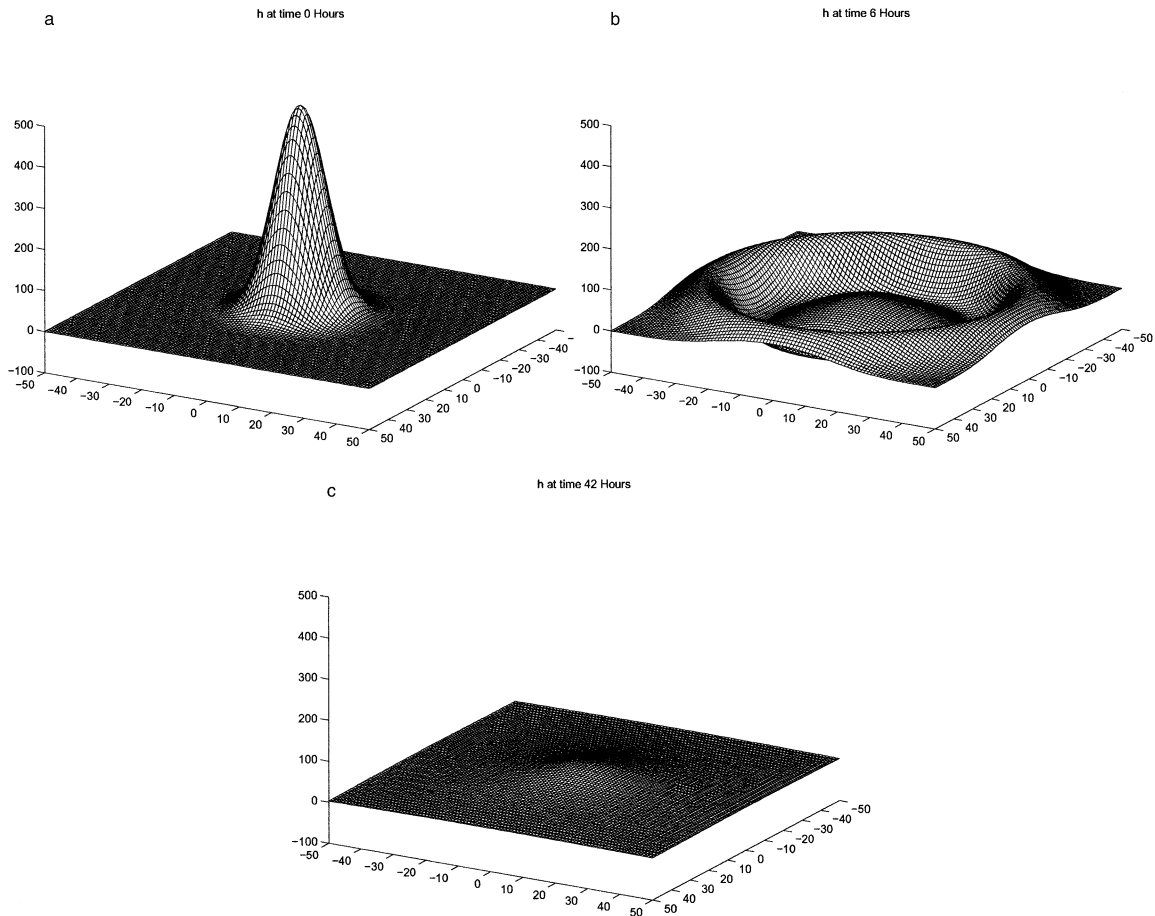
a   h at time 0 Hours

b   h at time 6 Hours

c   h at time 42 Hours

FIG. 1. The adjustment of a bell shape using PML absorbing boundary condition at (a) 0 h, (b) 6-h forecast, and (c) 42-h forecast.

b. Testing advection with PML

The linearized shallow water equations are given by (1)–(3) and have an analytic solution describing advection of a bell-shaped Gaussian with constant velocity (U, V) starting from the center of the domain at position (x_c, y_c). Thus we have an analytical solution to compare propagation of the Gaussian using the PML approach. The analytical solution for the bell-shaped Gaussian takes the form

$$\phi(x, y, t) = \Phi + \hat{\phi} \exp\left[-\left(\frac{x - x_c - Ut}{L_x/10}\right)^2\right]$$
$$\times \exp\left[-\left(\frac{y - y_c - Vt}{L_y/10}\right)^2\right], \qquad (17)$$

with (u, v) in geostrophic balance. As mentioned by

TABLE 2. Root-mean-square differences between a 48-h forecast and the asymptotic solution given by the balanced state.

Rms for h	Rms for u	Rms for v
0.64	0.01	0.01
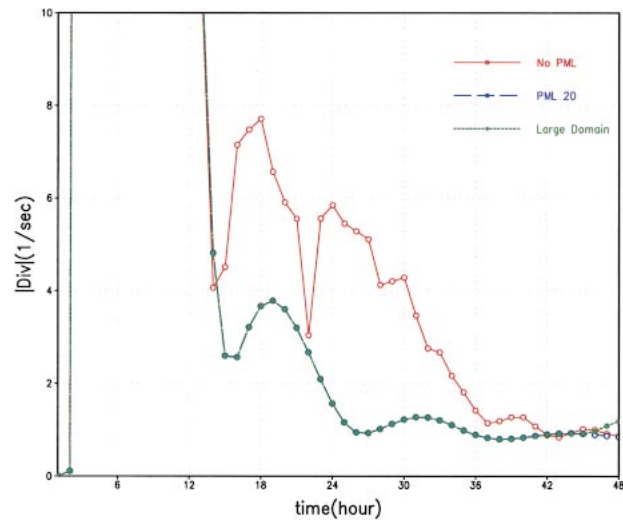
FIG. 2. Graph of the mean absolute divergence (s^{-1}) for the adjustment case multiplied by 10^8. Case of no PML, large computational domain, and a PML of 20-gridpoint thickness are displayed (in red, green, and blue, respectively).
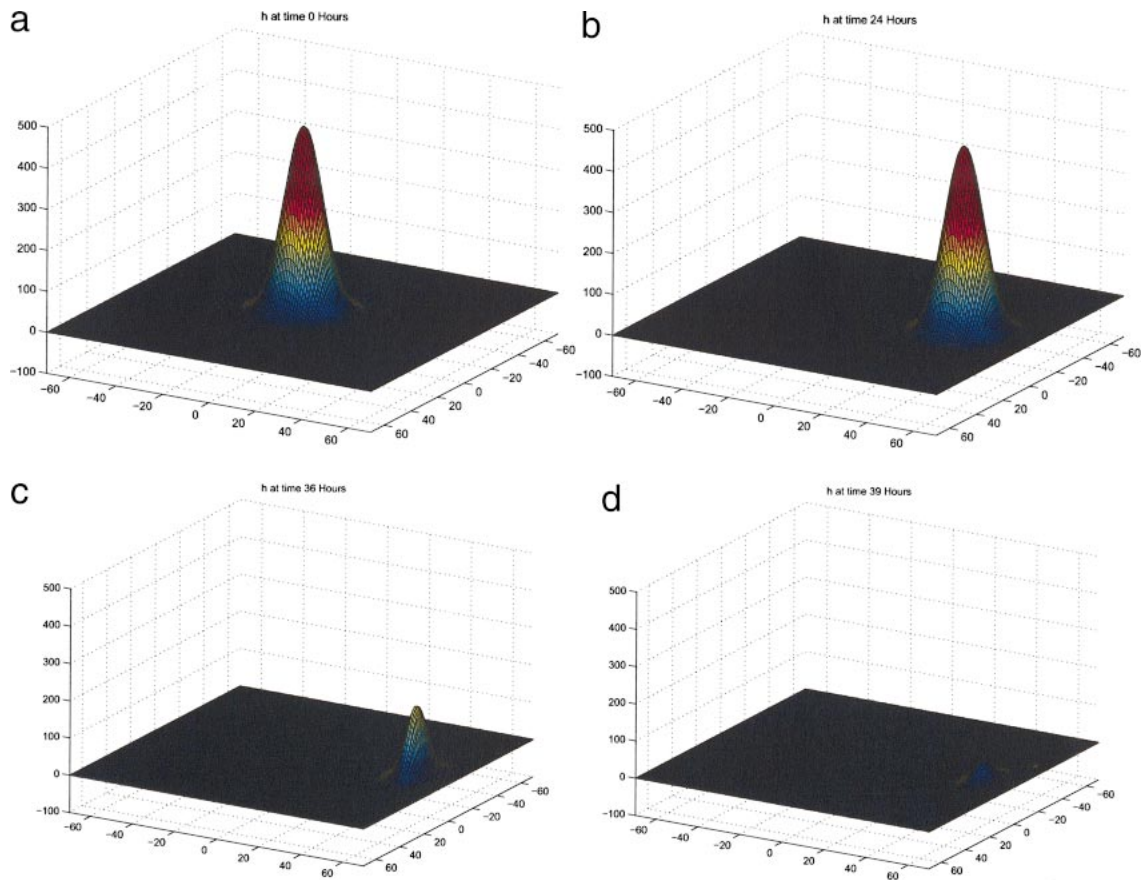
FIG. 3. The advection of a bell shape out of the computational domain moving parallel to PML x direction at (a) 0 h, (b) 24-h forecast, (c) 36-h forecast, and (d) 39-h forecast.

McDonald (2002) the analytic divergence is zero, and so this provides an additional test of the efficacy of the scheme used.

We tested the split PML for 2 cases: one is a wave propagating parallel to the x axis and the other at an angle of $45°$ with the x axis.

1) Propagation parallel to the PML x axis.

PML of 20 grid points, $U = 50$ m s^{-1}, $\sigma_m = 0.0018$, $\gamma = 3$, f plane and $\theta = 30°$, where θ is the latitude at which the Coriolis factor is calculated. A plot of the evolution of the advection of the bell-shaped Gaussian out of the area using the PML is provided. We display it for a period of integration of 39 h in Fig. 3. The figure shows that $h(x, y, t)$ is approximately a decaying translating Gaussian. We see that the PML layer is very effective and performs well as an absorbing boundary condition. The root-

TABLE 3. Root-mean-square difference between the 48-h forecast and the analytical solution.

Rms for h	Rms for u	Rms for v
2.27	0.30	0.50

mean-square difference between the 48-h forecast and the analytical solution is provided in Table 3.

A graph of the mean absolute divergence (in s^{-1}) multiplied by 10^8 for the propagation of the bell-shaped Gaussian for the case of propagation parallel to the PML is presented in Fig. 4. The results of all three cases coincide for the first 32 h. The results of the PML coincide with those of the large domain for the 48-h forecast whereas the results in the small region without PML show a big increase as the bell reaches the boundary (Fig. 4). As the bell reaches the boundary, the mean absolute divergence for the case without PML drastically increases, while the other two cases tend to nondivergence as in the analytical solution.

2) Propagation of the bell-shaped Gaussian at an angle of $45°$

We start with the bell-shaped Gaussian at the center of the domain and advect it so that it exits through a corner, that is, $(x_c, y_c) = (L_x/2, L_y/2)$ and $(U, V) = (50$ m s^{-1}, 50 m s$^{-1})$, thus ensuring that the Gaussian exits at the corner defined by (L_x, L_y).

In the implementation of the PML as an absorbing boundary condition we used a σ curve very similar
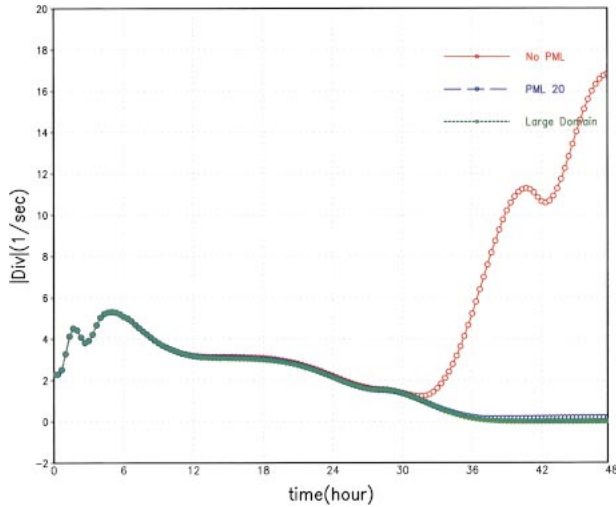
FIG. 4. Graph of the mean absolute divergence (s^{-1}) for the case of advection of a bell shape out of the computational domain moving parallel to PML multiplied by 10^8. Case of no PML, large computational domain, and a PML of 20-gridpoint thickness are displayed (in red, green, and blue, respectively).

to that used by Tam et al. (1998). The σ curve (see Fig. 5) starts with a value of $\sigma = 0$ at the fifth mesh point from the interface between the computational domain and the PML. It is then followed by eight mesh points where a cubic spline curve is used until the full value of $\sigma_x = \sigma_y = \sigma_m$ is attained. This was important for the case where artificial damping was used in the case where the bell was propagating at an angle.

We present graphically the generation of instabilities in the PML for this case. As a cure to instabilities manifested (confined) primarily to short waves, we applied a 9-point smoother in the PML:

$$u_{ij} \leftarrow \sum_{k=-1}^{1} \sum_{l=-1}^{1} \frac{u_{i+k\,j+l}}{2^{2+|k|+|l|}}. \tag{18}$$

Figure 6 shows the propagation of the Gaussian bell at an angle of 45°. We have shown the solution at 24 and 36 h. The initial solution is the same as in Fig. 3a. Since the advection speed is 50 m s^{-1} in each direction, the Gaussian bell is traveling along the diagonal from the center of the domain. Compare Fig. 6a to Fig. 3b. Figure 7 shows the 2D plot of the Gaussian bell propagating at an angle with and without a 9-point smoother after 60 h of forecast. Without the smoother the growth of the excited unstable solution spreads back into the interior computational domain (Fig. 7c), whereas using artificial damping provided by the 9 point Laplacian is effective in suppressing the instabilities of the PML equations. This filter continuously damps the instabilities once they propagate into the PML (Fig. 7b).

A graph of the mean absolute divergence (in sec^{-1}) multiplied by 10^8 for the propagation of the bell-shaped
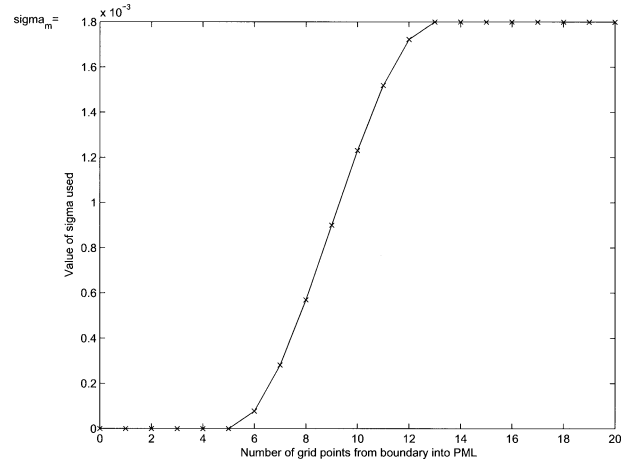

FIG. 5. Distribution of sigma within the PML layer for the case of bell propagation at an angle of 45°.

Gaussian for the case of propagation at an angle of 45° to the PML is presented in Fig. 8. The results agree up to $t = 34$ h and then display small variations probably due to the use of 9-point smoother.

4. Summary and conclusions

In this paper we have described and implemented the PML split-equations approach for the linearized shallow water equations based on an explicit Miller–Pearce finite-difference discretization scheme (see appendix of Miller and Pearce 1974).

The split-PML approach was tested for its efficiency as an absorbing boundary condition for the linearized shallow water equations using three different scenarios. First we tested permeability of the PML absorbing boundary conditions to adjustment waves. Measured against an asymptotic balanced state we found small rms errors for the 48-h forecast in the same range as those found by McDonald (2002). The rms between the 48-h forecast and the asymptotic solution are only slightly larger than those obtained in the best case of McDonald (2002). This may be attributed to our use of a grid-A model.

In a second scenario we tested the split PML for advection of the bell shape—viewed as a geostrophically balanced sharp pseudometeorological feature (McDonald 2002) for two separate cases, both starting with a bell-shaped Gaussian at the center of the computational domain:

1) The mean flow is parallel to the PML layer
2) Propagation at an angle of 45° exiting through a corner.

An analysis similar to that of Tam et al. (1998) finds that in such a case (i.e., propagation at an angle, when the mean flow is not unidirectional) the split PML for linearized shallow water equations supports unstable solutions. Application of a 9-point Laplacian filter stabi-
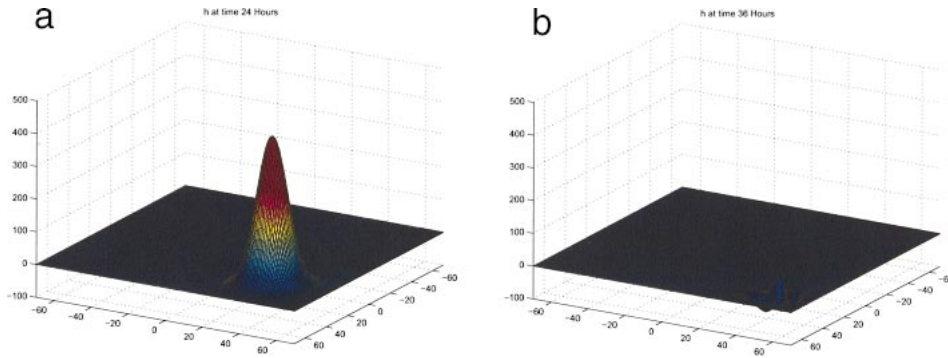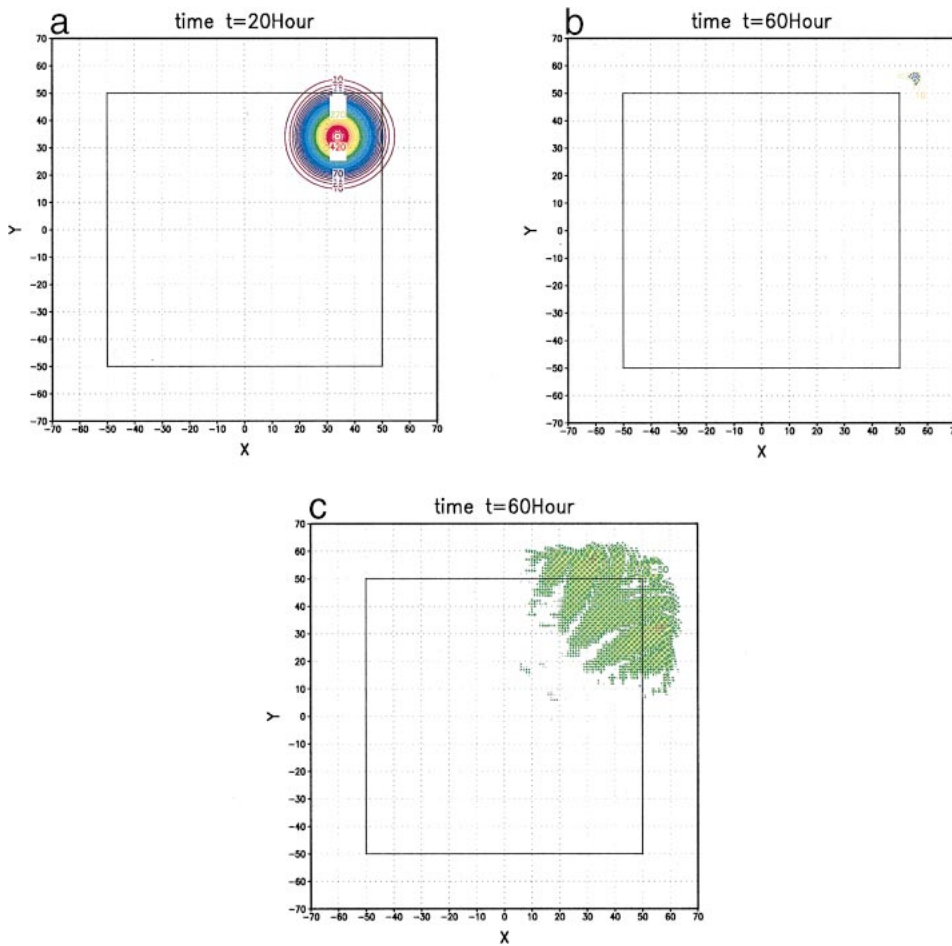
FIG. 6. The advection of a bell shape out of the computational domain moving at angle of 45° to PML x direction at (a) 24-h and (b) 36-h forecast.

lizes the PML. Our numerical experiments show that the stabilized PML performs well as an absorbing boundary condition for the linearized shallow water equations including the Coriolis factor. Our results com-

pare well with those obtained by McDonald (2002) for the same case.

The research carried out here has a natural extension to the formulation of boundary conditions for advanced

FIG. 7. The advection of the bell shape (2D) out of the computational domain moving at an angle of 45° to PML at (a) 20-h and (b) 60-h forecast using a 9 point filter. Simulation showing damping of unstable waves. (c) At 60-hour forecast without using the 9 point filter. Simulation showing propagation of unstable waves in the PML.
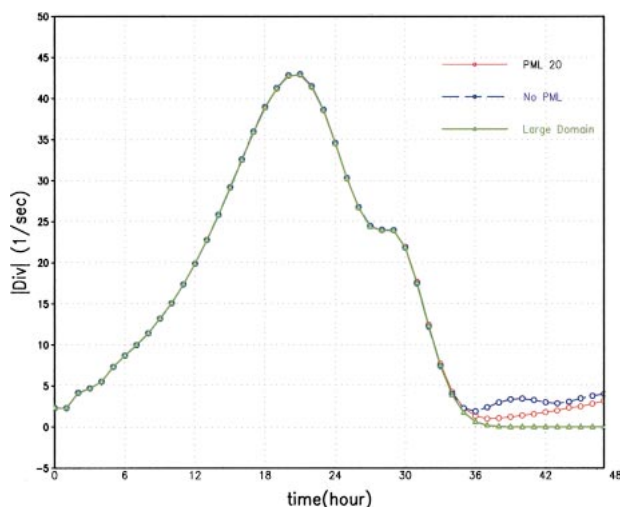
FIG. 8. Graph of the mean absolute divergence (s^{-1}) for the case of advection of a bell shape out of the computational domain moving at an angle of 45° to PML multiplied by 10^8. Case of no PML, large computational domain, and a PML of 20-gridpoint thickness are displayed (in red, green, and blue, respectively).

mesoscale models, such as the fifth-generation Pennsylvania State University–National Center for Atmospheric Research Mesoscale Model (MM5) and the new Medium-Range Forecast (MRF) models, and may improve upon the combination of nudging and sponge layer approches presently used in such models. Work with PML in the framework of mesoscale models will mean that gravity waves can not only leave the domain but can also enter it without hindrance (McDonald 2003).

Our results are encouraging and constitute a step toward using the PML absorbing boundary conditions for full 3D atmospheric and ocean models. One avenue to achieve this goal is to implement the PML boundary conditions in a 3D multilayer shallow water equations model as a way to proceed toward full 3D models. This can be done for the linearized hydrostatic equations by carrying out a normal-mode decomposition yielding a shallow water equation for each vertical mode.

Development of a nonsplit version of both the linearized and the nonlinear version of the shallow water equations based on ideas put forward by Abarbanel and Gottlieb (1998), Abarbanel et al. (1999), and Hesthaven (1998) is presently also being investigated.

REFERENCES

Abarbanel, S., and D. Gottlieb, 1997: A mathematical analysis of the PML method. *J. Comput. Phys.,* **134,** 357–363.
——, and ——, 1998: On the construction and analysis of absorbing layers in CEM. *Appl. Numer. Math.,* **27,** 331–340.
——, ——, and J. S. Hesthaven, 1999: Well-posed perfectly matched layers for advective acoustics. *J. Comput. Phys.,* **154,** 266–283.
Berenger, J.-P., 1994: A perfectly matched layer for the absorption of electromagnetic waves. *J. Comput. Phys.,* **114,** 185–200.
Clement, A., 1996: Coupling of two absorbing boundary conditions for 2D time-domain simulation of free surface gravity waves. *J. Comput. Phys.,* **126,** 139–151.
Collino, F., 1997: Perfectly matched absorbing layers for paralaxial equations. *J. Comput. Phys.,* **131,** 164–180.
Darblade, G., 1997: Methodés numériqués et conditions aux limites pour les modèles shallow water multicouches. Ph.D. thesis, Université de Bordeaux I, 225 pp. [Available from Prof. A. Y. LeRoux, Institut de Mathématiques, Université Bordeaux I, F-33405 Talence, France.]
——, R. Baraille, A.-Y. le Roux, X. Carton, and D. Pinchon, 1997: Conditions limites non réfléchissantes pour un modèle de Saint-Venant bidimensionnel barotrope linéarisé. *C. R. Acad. Sci. Paris,* **324,** 485–490.
Davies, H. C., 1976: A lateral boundary formulation for multilevel prediction models. *Quart. J. Roy. Meteor. Soc.,* **102,** 405–418.
——, 1983: Limitations of some common lateral boundary schemes used in regional NWP models. *Mon. Wea. Rev.,* **111,** 1002–1012.
Engquist, B., and A. Majda, 1977: Absorbing boundary conditions for the numerical simulation of waves. *Math. Comput.,* **31,** 629–651.
——, and ——, 1979: Radiation boundary conditions for acoustic and elastic wave calculations. *Commun. Pure. Appl. Math.,* **32,** 313–357.
Gill, A. E., 1982: *Atmosphere–Ocean Dynamics.* Academic Press, 662 pp.
Givoli, D., 1991: Nonreflecting boundary conditions. *J. Comput. Phys.,* **94,** 1–29.
——, and J. B. Keller, 1989: A finite element method for large domains. *Comput. Methods Appl. Mech. Eng.,* **76,** 41–66.
Gustafsson, B., and A. Sundström, 1978: Incompletely parabolic problems in fluid dynamics. *SIAM J. Appl. Math.,* **35,** 343–357.
Hayder, M. E., and H. L. Atkins, 1998: Experience with PML boundary conditions in fluid flow computation. *IUTAM Symposium on Computational Methods for Unbounded Domains,* T. L. Gears, Ed., Kluwer Academic, 207–216.
——, F. Q. Hu, and M. Y. Hussaini, 1999: Towards perfectly absorbing boundary conditions for Euler equations. *AIAA J.,* **37,** 912–918.
Hesthaven, J. S., 1998: On the analysis and construction of perfectly matched layers for the linearized Euler equations. *J. Comput. Phys.,* **142,** 129–147.
Holstad, A., and I. Lie, 2001: Transparent boundary conditions using a mixed finite element formulation of the shallow water equations. Norwegian Meteorological Institute (DNMI) Research Rep. 120, 48 pp.
Hu, F. Q., 1996a: On absorbing boundary conditions for linearized

Euler equations by a perfectly matched layer. *J. Comput. Phys.,* **129,** 201–219.

——, 1996b: On a perfectly matched layer as an absorbing boundary condition. AIAA Paper 96-1664, 17 pp.

——, 2001: A stable, perfectly matched layer for linearized Euler equations in unsplit physical variables. *J. Comput. Phys.,* **173,** 455–480.

Kalnay, E., 2001: *Numerical Weather Forecasting and Predictability.* Cambridge University Press, 364 pp.

Kar, S. K., and R. P. Turco, 1995: Formulation of a lateral sponge layer for the limited-area shallow-water models and an extension for the vertically stratified case. *Mon. Wea. Rev.,* **123,** 1542–1559.

Karni, S., 1996: Far field filtering operators for suppression of reflections from artificial boundaries. *SIAM J. Numer. Anal.,* **33,** 1014–1047.

Kosloff, R., and D. Kosloff, 1986: Absorbing boundaries for wave propagation problems. *J. Comput. Phys.,* **63,** 363–376.

Lie, I., 2001: Well-posed transparent boundary conditions for the shallow water equations. *Appl. Numer. Math.,* **38,** 445–474.

McDonald, A., 1997: Lateral boundary conditions for operational regional forecast models: A review. HIRLAM Tech. Rep. 32, 31 pp.

——, 2000: Boundary conditions for semi-Lagrangian schemes: Testing some alternatives in one-dimensional models. *Mon. Wea. Rev.,* **128,** 4084–4096.

——, 2001a: A step toward transparent boundary conditions for meteorological models. HIRLAM Tech. Note 57, 22 pp.

——, 2001b: Well posed boundary conditions for semi-Lagrangian schemes: The two dimensional case. HIRLAM Tech. Rep. 47, 38 pp.

——, 2002: A step toward transparent boundary conditions for meteorological models. *Mon. Wea. Rev.,* **130,** 140–151.

——, 2003: Transparent boundary conditions for the shallow water equations: Testing in a nested environment. *Mon. Wea. Rev.,* **131,** 698–705.

Metral, J., and O. Vacus, 1999: Well-posedness of the Cauchy problem associated with Berenger's system. *C. R. Acad. Sci. Paris Ser. I,* **328,** 847–852.

Miller, M. J., and R. P. Pearce, 1974: A three dimensional primitive equation model of cumulonimbus convection. *Quart. J. Roy. Meteor. Soc.,* **100,** 133–154.

Rahmouni, A., 2000: A well-posed unsplit PML model for linearized Euler equations. *C. R. Acad. Sci. Paris Ser. I,* **331,** 159–164.

Tam, C. K. W., L. Aurialt, and F. Cambuli, 1998: Perfectly matched layer as an absorbing boundary condition for the linearized Euler equations in open and ducted domains. *J. Comput. Phys.,* **144,** 213–234.

Tsynkov, S. V., 1998: Numerical solution of problems on unbounded domains: A review. *Appl. Numer. Math.,* **27,** 465–532.

Turkel, E., 1983: Progress in computational physics. *Comput. Fluids,* **11,** 121–144.